Chemistry–A European Journal

Supporting Information

Taming the Lewis Superacid $Al(ORF)_3$ ($RF = C(CF_3)_3$): DFT Guided Identification of the "Stable yet Reactive" Adduct $SiPr_2 \rightarrow Al(ORF)_3$; Its Use as ORF- Abstractor from a "Ni-ORF" complex

Julien Petit, Julien Babinot, Nathalie Saffon-Merceron, Lionel Magna,* and Nicolas Mézailles*

Table of contents

1. Experimental procedures and NMRs

Reagents and solvents

All the reactions were carried out in a glove box or using standard Schlenk techniques under N_2. All commercial compounds were put under inert atmosphere before use. Compound **3**, $(bipyMe_2)Ni(OR^F)_2$, was synthesized according to our previously reported procedure.[1] All solvents, except o-DFB, were taken from MBSPS-800 solvent purification system, then degassed and further dried using molecular sieves. *o*-DFB was pre-dried over CaH_2 and then filtered and stored on molecular sieves.

NMR

^1H, ^{13}C, ^{19}F and ^{31}P NMR spectra were recorded on Bruker Avance 300 and 400 MHz spectrometers. ^1H and ^{13}C chemical shifts reported are referenced internally to used solvent while ^{19}F and ^{31}P chemical shifts are referenced to an external standard of trichlorofluoromethane and phosphoric acid respectively.

Elemental analysis (C, H, N)

Elemental analysis of **1-S^{i}Pr$_2$** powder was carried out by combustion analysis using vario MICRO cube apparatus from Elementar.

HRMS

HRMS analyses were conducted with "QTOF Impact II - Bruker / UHPLC U3000 chain – Dionex" spectrometer. A cryospray (Cold Spray Ionization) source is used to detect exact masses.[2]

XRD analysis

X-ray intensity data were collected at 193 K on a Bruker-AXS D8-VENTURE diffractometer (**4, 1-S^{i}Pr2, 1-OPEt3, 5, 5-H$_2$O, 6[Al(OR^F)4]** and **8**) equipped with a Mo Kα sealed tube (λ = 0.71073 Å), a multilayer TRIUMPH X-Ray mirror and a Photon III-C14 detector or at 153 K on a Bruker-AXS kappa APEX II Quazar diffractometer (**6[Al-F-Al]**) equipped with a 30W air-cooled microfocus source using Mo Kα radiation (**8**). The semi-empirical absorption corrections were employed.[3] The structures were solved using an intrinsic phasing method,[4] and refined by full matrix least squares procedures on F^2.[4] All non-H atoms were refined with anisotropic displacement parameters. Hydrogen atoms were refined isotropically at calculated positions using a riding model with their isotropic displacement parameters constrained to be equal to 1.5 times the equivalent isotropic displacement parameters of their pivot atoms for terminal sp3 carbon and 1.2 times for all other carbon atoms. Crystallographic data and refinement details are given in **2**.

In all these structures, a large part of the molecule were disordered. Several restraints (SAME, SADI, SIMU, DELU, ISOR) were applied to refine some moieties of the molecules and to avoid the collapse of the structures during the least-squares refinement by the large anisotropic displacement parameters. Some bond lengths were restrained with DFIX to suitable target values (**6[Al(OR^F)4]**). H atoms on O (**5-H$_2$O**) were located by difference Fourier map and were freely refined. The obtained crystals of **4** were small, very weakly diffracting and were found to be non-merohedrally twinned. The TwinRotMat routine in the PLATON program[5] was used to determine the twin laws and the data generated were used in the final refinement. This structure only allowed us to identify complex 4, the overall quality of this structure is too poor to show bond distances and angles.

CCDC-2218595 (**4**), CCDC-2218596 (**1-S^{i}Pr2**), CCDC-2218597 (**1-OPEt3**), CCDC-2218598 (**5**), CCDC-2218599 (**5-H$_2$O**), CCDC-2218600 (**6[Al(OR^F)4]**), CCDC-2218601 (**6[Al-F-Al]**) and CCDC-2218602 (**8**) contain the supplementary crystallographic data. These data can be obtained free of charge from https://www.ccdc.cam.ac.uk/structures/ or from the Cambridge Crystallographic Data Centre, 12

Union Road, Cambridge CB2 1EZ, UK; tel: + 44 (0)1223 336408; fax: + 44 (0)1223336033; or e-mail: deposit@ccdc.cam.ac.uk

Syntheses

Synthesis of ($^{i}Pr_2S$)→Al(OR^F)$_3$ **1-S^{i}Pr$_2$**:

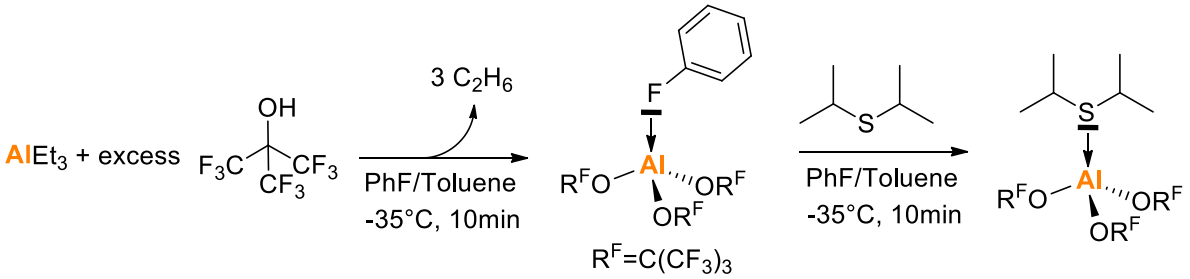

A solution of per-fluoro-tert-butanol (0.65mL, 4.66mmol, 4.9 eq.) in fluorobenzene (3mL) was added at -20°C onto a solution of $AlEt_3$ (0.5ml, 1.9M in toluene, 0.95mmol, 1 eq.) in fluorobenzene (3mL). A gas release was observed at once (ethane). The mixture was allowed to react 10min at -35°C. A solution of di-isopropyl sulphide (0.15 mL, 1.03mmol, 1.1 eq.) in fluorobenzene (2mL) was added to the previous mixture, still at -35°C. The mixture was allowed to warm up to RT. Solvent was removed under reduced pressure which removed both the excess of $S^{i}Pr_2$ and the excess of alcohol. The obtained white solid (750mg, 93%) does not need further purification as attested by the results of the elemental analysis and can be stored at RT under inert atmosphere for a long period (months). Crystals were obtained from a saturated solution in toluene or from diffusion of heptane in a solution of the compound in fluorobenzene.

^{1}H NMR (298K, 300,0MHz, C_6D_6): 0.94 (d, J=6.90Hz, 12H, CH_3), 3.22 (sept., J=6.90Hz, 2H, C**H**Me_2) ppm. **^{13}C{^{1}H}{^{31}P} NMR** (298K, 75 MHz, C_6D_6): 22.23 (s, CH_3), 39.06 (s, CH), 121.32 (q, $J_{C\text{-}F}$=292Hz, CF_3) ppm. **^{19}F{^{1}H} NMR** (298K, 282 MHz, C_6D_6): -74.8 (s, $C(CF_3)_3$) ppm. **EA**: Anal. Calc for $C_{18}H_{14}AlF_{27}O_3S$: C, 25.43; H, 1.66. Found: C, 25.19; H,1.17.

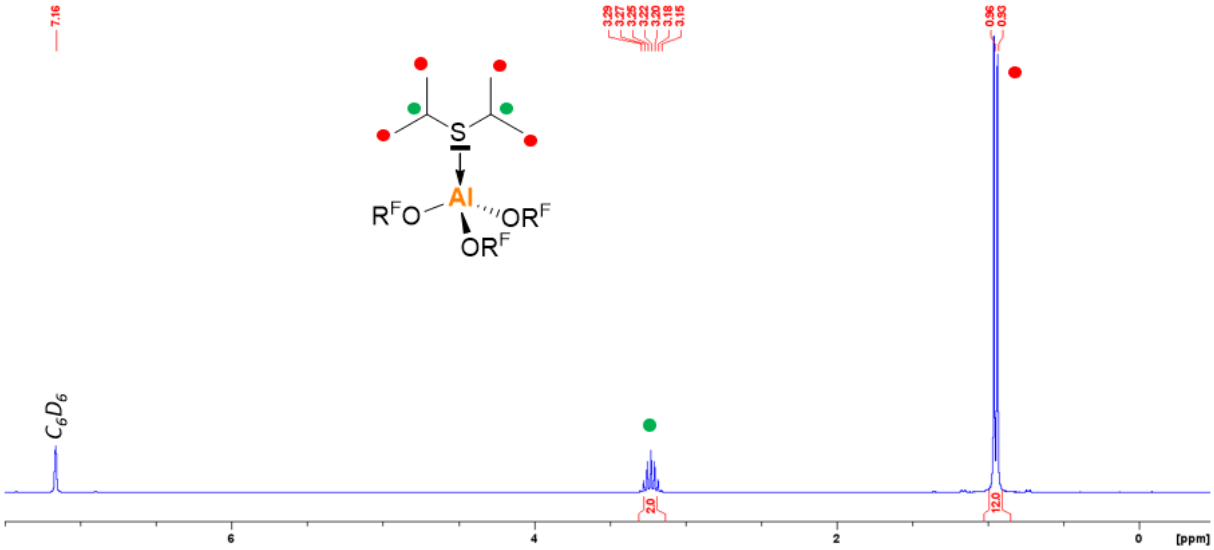

Figure S1 – ^{1}H NMR (300MHz, 298K) of **1-S^{i}Pr$_2$** at 25°C in C_6D_6.

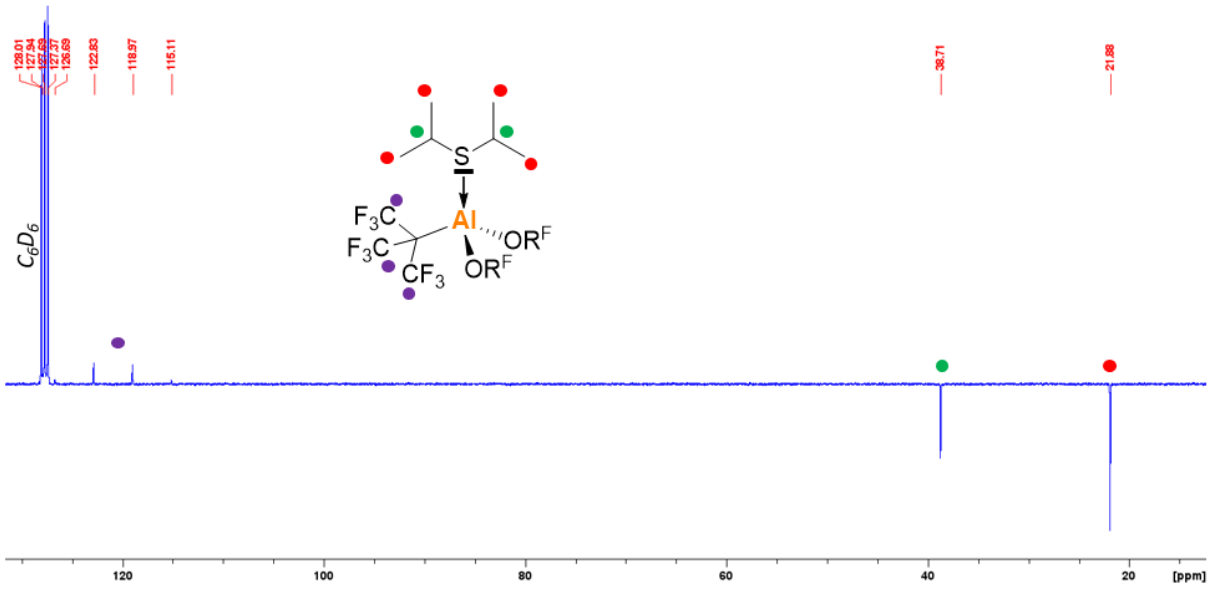

Figure S2 – ^{13}C NMR (75MHz, 298K) of **1-S^{i}Pr$_2$** at 25°C in C_6D_6.

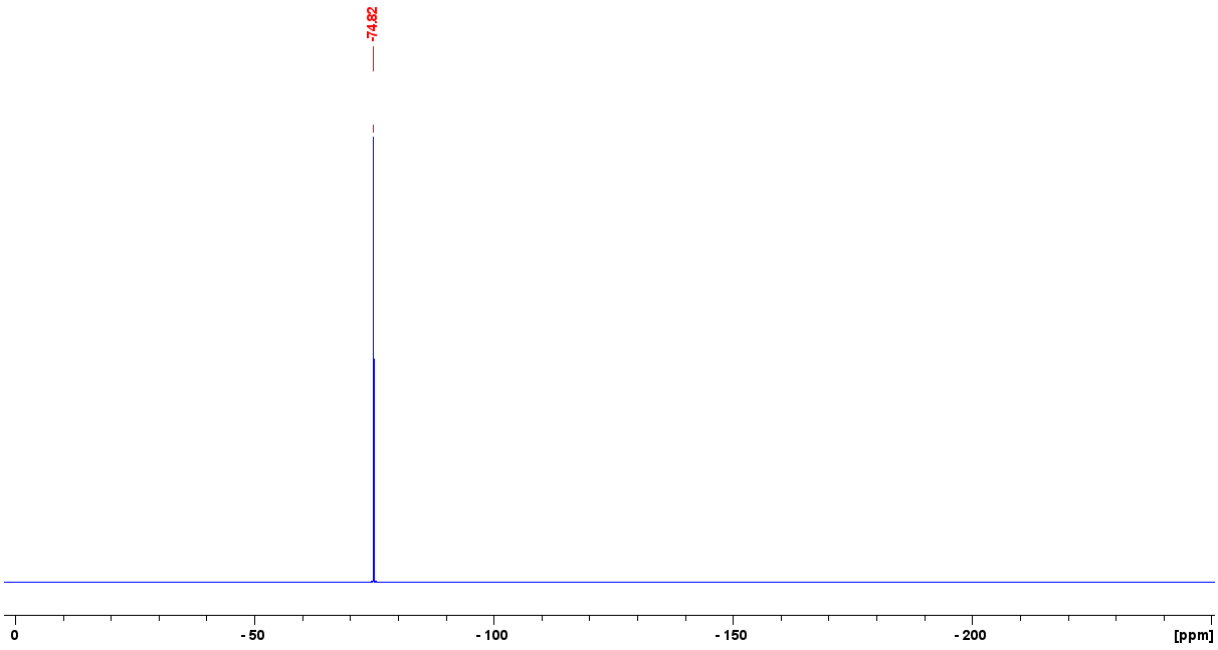

Figure S3 – $^{19}F\{^1H\}$ NMR (282MHz, 298K) of **1-S^{i}Pr$_2$** at 25°C in C_6D_6.

Synthesis of $(Et_3PO) \rightarrow Al(OR^F)_3$ **1-OPEt$_3$**:

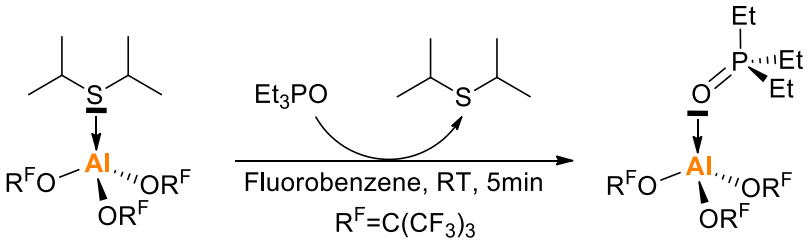

A solution of Et_3PO (15.8mg, 0.12mmol, 1eq.) in fluorobenzene (5mL) was added onto a solution of (iPr$_2$S)→Al(ORF)$_3$ (100mg, 0.12mmol, 1eq.) in fluorobenzene (5mL). The mixture was allowed to react 30min at RT. Solvent was then removed under reduced pressure to afford a white solid which was

extensively dried under reduced pressure. The obtained white solid (92mg, 90%) does not need further purification and can be stored at RT under inert atmosphere for long periods (months). Crystals were obtained from a saturated solution of deuterated benzene.

^{1}H NMR (298K, 500MHz, CD_2Cl_2): 1.20 (d of t, J_{HH}=7.7 Hz, J_{PH}=18.5 Hz, 9H, CH_3), 1.95 (d of q, J_{HH}=7.7 Hz, J_{PH}=11.8 Hz, 6H, CH_2) ppm. **^{13}C{^{1}H} NMR** (298K, 125.7 MHz, CD_2Cl_2): 4,68 (d, $J_{C\text{-}P}$=5.1 Hz CH_3), 17.94 (d, $J_{C\text{-}P}$=66.5 Hz, CH_2) 121.59 (q, $J_{C\text{-}F}$=292Hz, CF3) ppm. **^{19}F NMR** (298K, 470.6 Hz, CD_2Cl_2): -75.6 (s, $C(CF_3)_3$) ppm. **^{31}P{^{1}H} NMR** (298K, 121.5 Hz, CD_2Cl_2): 78.0 (s) ppm. **HRMS** (TOF): Calc. for $(Et_3PO)Al(ORF)_2$ = $C_{14}H_{15}AlO_3F_{18}P$ 631.0287 ; found 631.0291.

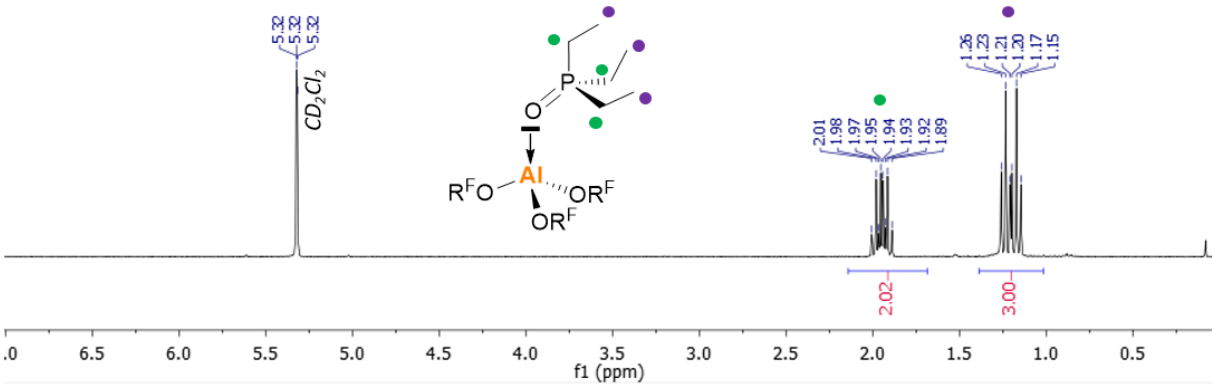

Figure S4 – ^{1}H NMR (500MHz, 298K) of **1-OPEt$_3$** at 25°C in CD_2Cl_2.

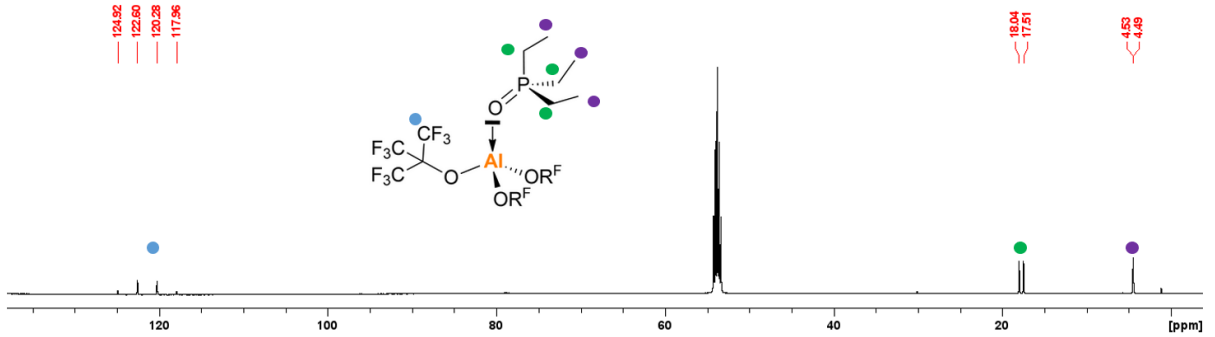

Figure S5 - ^{13}C NMR (125MHz, 298K) of **1-OPEt$_3$** at 25°C in CD_2Cl_2.

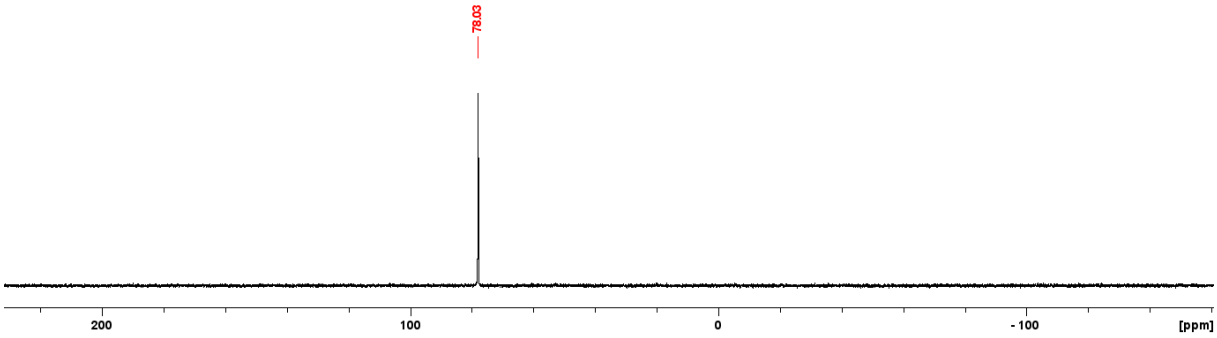

Figure S6 – ^{31}P{^{1}H} NMR (202MHz, 298K) of **1-OPEt$_3$** at 25°C in CD_2Cl_2.

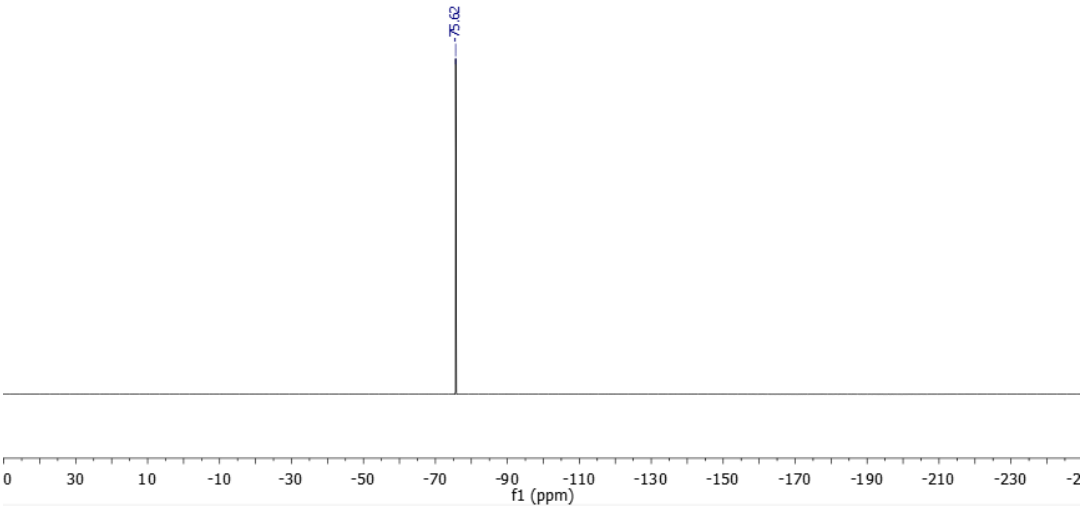

Figure S7 – $^{19}F\{^{1}H\}$ NMR (470.4 MHz, 298K) of **1-OPEt$_3$** at 25°C in CD_2Cl_2.

Formation of dimer $[(R^FO)_2Al(OEt)]_2$ **4** :

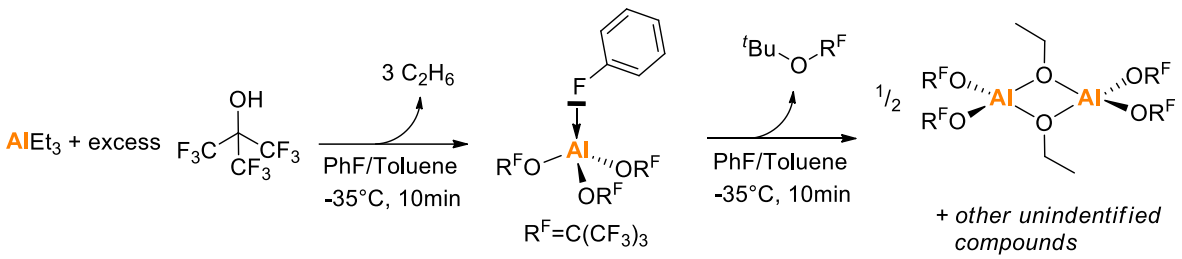

A solution of $AlEt_3$ in toluene (1.9M, Aldrich, 0.5mL, 0.95mmol, 1eq.) was mixed with fluorobenzene (5mL). This colorless solution was cooled down to -35°C. A solution of R^FOH (0.41mL, 2.95mmol, 3.1eq.) in fluorobenzene (5mL) was then added. A gas released was observed (C_2H_6) and solution remained colorless. After 10min at -30°C, ^{t}BuOEt (excess) was added. The mixture was then allowed to warm up until RT. 1 mL of the solution was taken for NMR analyses. The rest was concentrated to 4 mL and allowed to rest at 5°C. After one day, colorless crystals of compound **4** were collected on the side of the Schlenk tube and analyzed by XRD.

Synthesis of $[(bipyMe_2)Ni(OR^F)(S^iPr_2)][Al\text{-}F\text{-}Al]$ **5** :

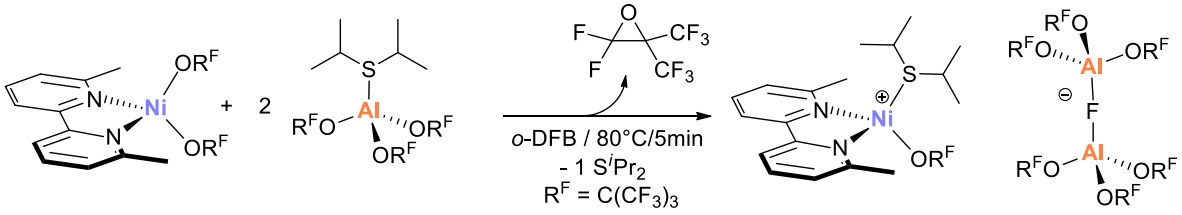

To a solution of (6 6'-dimethyl-2,2'-bipyridine)$Ni(OR^F)_2$ (100 mg, 0.14 mmol, 1eq.) in *o*-DFB (3mL), a solution of $(S^iPr_2)Al(OR^F)_3$ (238.5 mg, 0.28 mmol, 2eq.) in *o*-DFB (3mL) was added dropwise. The mixture was heated at 80°C during 5min. The solution, which remained orange, was concentrated to 2mL. A layer of HMDSO (3mL) was slowly added on the crude mixture. After 48h of diffusion at 25°C, deep red crystals suitable for X-Ray diffraction analyses were obtained.

^{1}H NMR (298K, 300,0MHz, *o*-DFB): -2.22 – 2.77 (br, S^iPr_2, n x 14H), 16.08 (s, $bipyMe_2$-ArH, 2H), 37.70 (br, $bipyMe_2$-CH_3, 6H), 55.11 (s, $bipyMe_2$-ArH, 2H) 82.59 (s, $bipyMe_2$-ArH, 2H) ppm **$^{19}F\{^1H\}$ NMR** (298K, 282,2 Hz, *o*-DFB): +52 (s, Ni-O-C$(CF_3)_3$, 9F), -75 (s, Al-O-C$(CF_3)_3$, 54F), -184ppm (br, Al-**F**-Al, 1F) ppm.

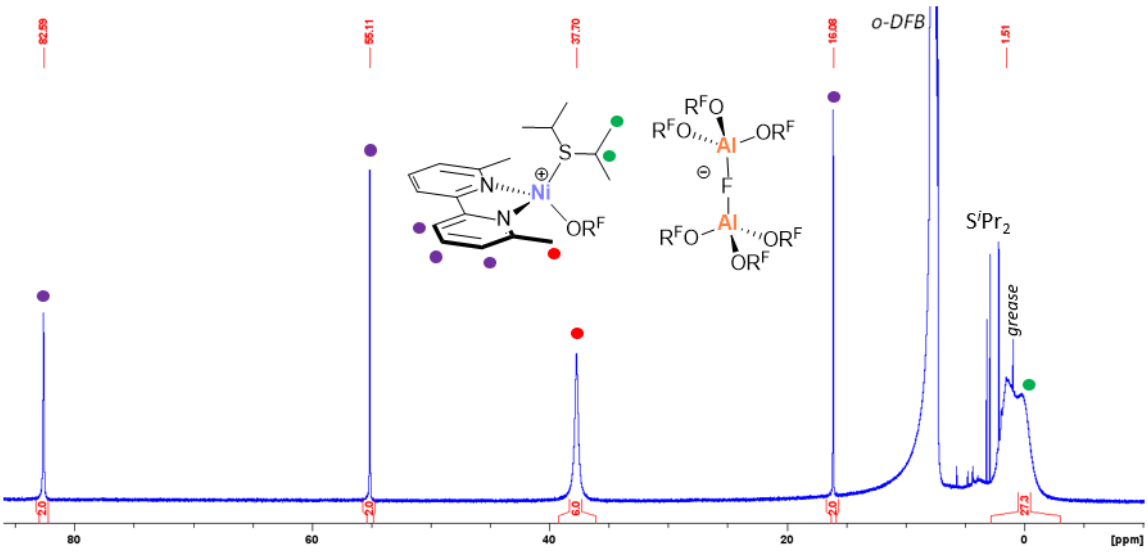

Figure S8 – ^{1}H NMR (300MHz, 298K, *o*-DFB) of **5** (crude mixture obtained after addition of 2eq. of **2** on (bipyMe$_2$)Ni(OR^F)$_2$ in *o*-DFB at 80°C during 5 min) at 25°C in *o*-DFB.

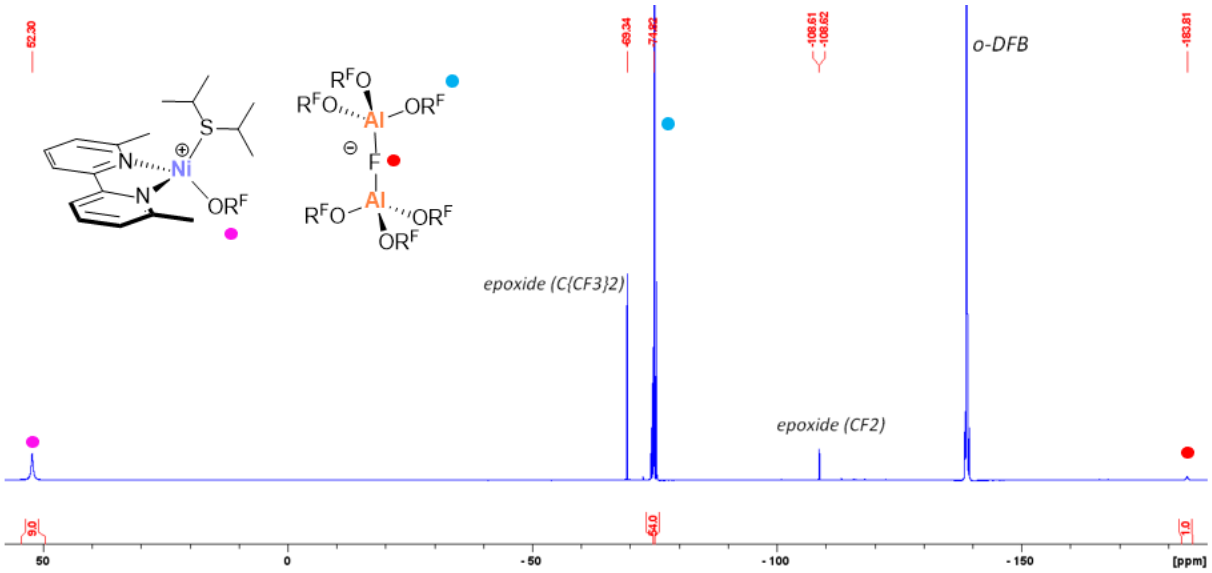

Figure S9 – ^{19}F{^{1}H} NMR (282MHz, 298K, *o*-DFB) of **5** (crude mixture obtained after addition of 2eq. of **2** on (bipyMe$_2$)Ni(OR^F)$_2$ in *o*-DFB at 80°C during 5 min) at 25°C in *o*-DFB. Epoxide = O(CF$_2$)(C{CF$_3$}$_2$).

Synthesis of [(bipyMe$_2$)Ni(OR^F)(PPh$_3$)][Al-F-Al] **6$^+$[Al-F-Al]** :

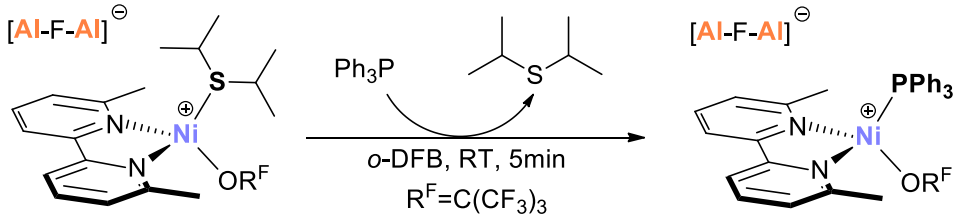

To a solution of (6,6'-dimethyl-2,2'-bipyridine)Ni(OR^F)$_2$ (100mg, 0.14 mmol, 1eq.) in *o*-DFB (3mL), a solution of (S^{i}Pr$_2$)Al(OR^F)$_3$ (238.5 mg, 0.28 mmol, 2eq.) in *o*-DFB (3mL) was added dropwise. The mixture was heated at 80°C during 5min. A solution of Ph$_3$P (36.8 mg, 0.14 mmol, 1 eq.) in *o*-DFB (3mL) was added on the previous mixture. The solution became bright yellow at once. The solution was concentrated to 2mL and a layer of HMDSO (3mL) was slowly added. After 48h of diffusion at 25°C, deep red crystals suitable for X-Ray diffraction analyses were obtained.

^{1}H NMR (298K, 300,0MHz, *o*-DFB): -8.36 – -4.84 (br, Ph_3P-ArH, 10H), 17.95 (br, bipyMe_2-CH_3, 6H), 22.70 (br, Ph_3P-Ar-H, 5H), 45.48 (s, bipyMe_2-ArH, 2H), 75.22 (s, bipyMe_2-ArH, 2H) ppm **^{19}F{^{1}H} NMR** (298K, 282,2 Hz, *o*-DFB): +105 (s, Ni-O-C$(CF_3)_3$, 9F), -75 (s, Al-O-C$(CF_3)_3$, 54F), -184ppm (br, Al-**F**-Al, 1F) ppm. **HRMS** (CSI): calc. for $[(bipyMe_2)Ni(OR^F)(PPh_3)]^+$= $C_{34}H_{27}F_9N_2NiOP^+$ 739.1066 ; found 739.1067.

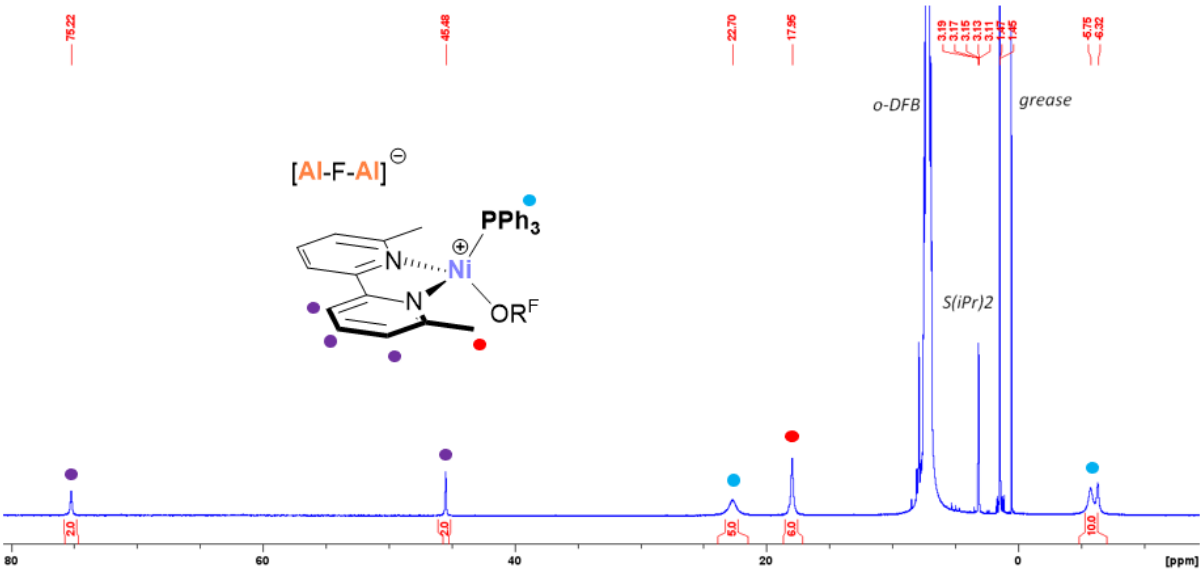

Figure S10 - ^{1}H NMR (300MHz, 298K, *o*-DFB) of **6$^+$[Al-F-Al]** at 25°C in *o*-DFB (crude mixture obtained after addition of 1eq. of PPh_3 on **4** in *o*-DFB).

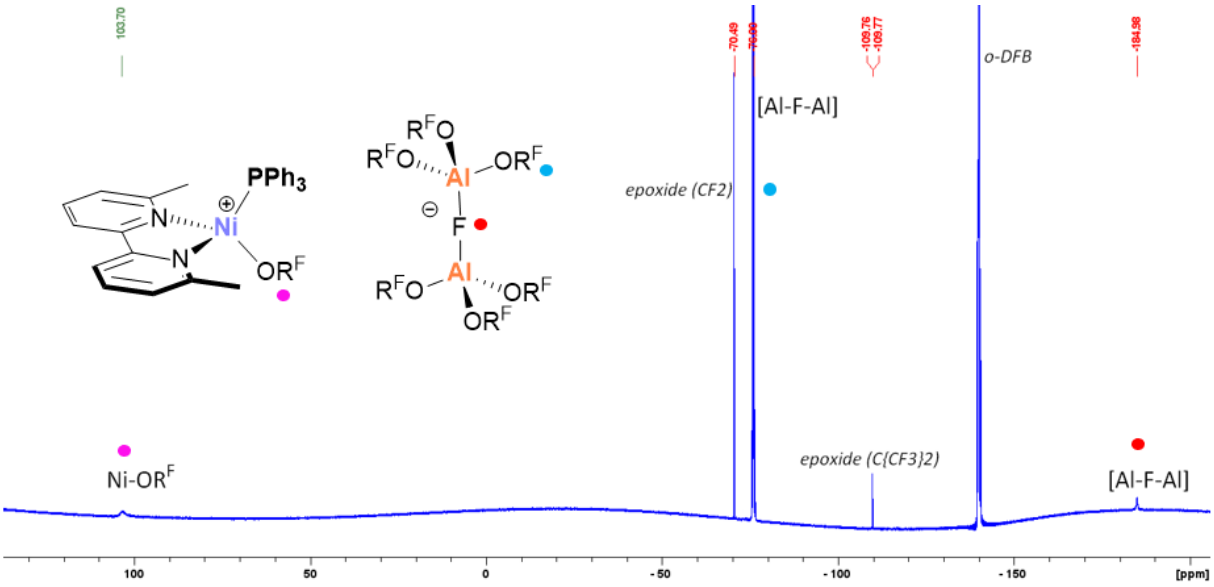

Figure S11 - ^{19}F{^{1}H} NMR (282MHz, 298K, *o*-DFB) of **6$^+$[Al-F-Al]** at 25°C in *o*-DFB (crude mixture obtained after addition of 1eq. of PPh_3 on **5** in *o*-DFB). Epoxide = $O(CF_2)(C\{CF_3\}_2)$.

Partial evolution of complex **6**$^{+}$[AlFAl]$^{-}$ to **6**$^{+}$[Al(OR^{F})$_4$]$^{-}$ in o-DFB at room temperature:

Surprisingly, over time, major rearrangements occurred within the counter anion of the complex. Following the addition of PPh_3 reaction by ^{19}F NMR showed that the expected, complex **6**$^{+}$[AlFAl]$^{-}$ (δ -76.00 ppm) was the only species only after mixing. Within 24 hours at room temperature, new signals were observed at -75.86 ppm and -75.76 ppm, which intensified with time (see ESI, figure S11). In parallel, a new signal at -184 ppm appeared next to the signal at -185 ppm of [Al-F-Al]$^{-}$. This new signal associated to the signal at -75.76 ppm corresponds to the known cyclic compound **2** (**Erreur ! Source du renvoi introuvable.**), while the one at -75.86 ppm is due to the counter-anion [Al(OR^{F})$_4$]$^{-}$. Yellow crystals were obtained from the mixture after two weeks (HMDSO/*o*-DFB, RT). X-ray diffraction analysis of these crystals showed that cation **6+** is now associated to the [Al(OR^{F})$_4$]$^{-}$ counter anion (see **Figure S17** and **Figure S18**). This transformation was very surprising as this reactivity has never been reported with other cations (Ag^{+}, Ni^{+}, Sn^{2+}, Ga^{+})[6–10] or for complex [(bipyMe$_2$)Ni(OR^{F})(S^{i}Pr$_2$)] **5**$^{+}$[AlFAl]$^{-}$.[11]

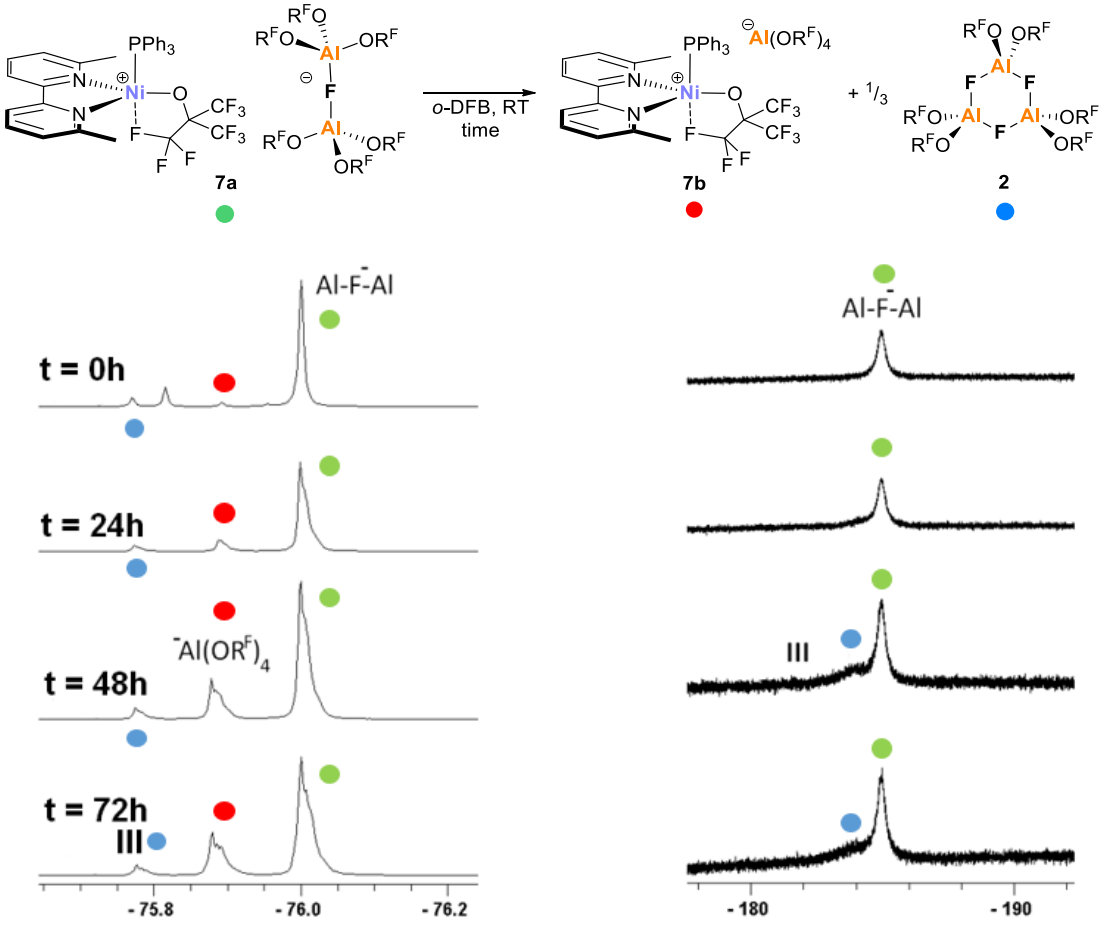

Figure S12 – From **6**$^{+}$**[Al-F-Al]** to **6**$^{+}$**[Al(OR^{F})$_4$]**: evolution of ^{19}F NMR signals over time in the [-76.2; -75.5] (left) and [-191; -179] (right) regions.

Synthesis of complex $[(R^FO_3Al)(\mu\text{-}Cl)(bipyMe_2Ni)(\mu\text{-}Cl)]_2$ **8**:

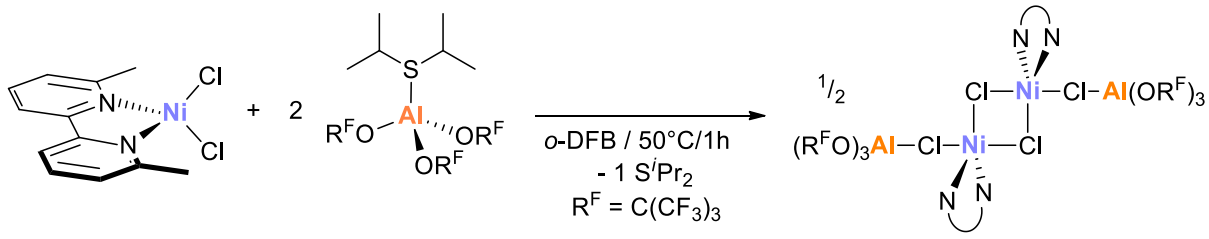

A solution of **1-S^{i}Pr$_2$** (271mg, 0.32mmol, 1eq.) in *o*-DFB (3mL) was added onto a suspension $(bipyMe_2)NiCl_2$ (100mg, 0.32mmol, 1eq.) in *o*-DFB (3mL). The mixture was heated at 50°C for 1h under stirring. A deep orange solution was obtained (NMRs of the crude presented below). The solution was concentrated to ½ of its initial volume and HMDSO was added for diffusion. After one day, deep orange crystals had formed and were analyzed by X-Ray diffraction. Upon dissolution of the crystals for analysis purposes in *o*-DFB, ^{1}H NMR show several "$(bipyMe_2)Ni$" fragments. On the other hand, unidentified signals around -75ppm are systematically observed in ^{19}F NMR.

^{1}H NMR (298K, 300,0MHz, *o*-DFB): 16.32 (br, Ar-H), 24.07 (br, CH_3), 57.00 (br, Ar-H), 79.11 (br, Ar-H) ppm. **^{19}F NMR** (298K, 282,2 Hz, *o*-DFB): -76 (s, Al-O-C$(CF_3)_3$) ppm.

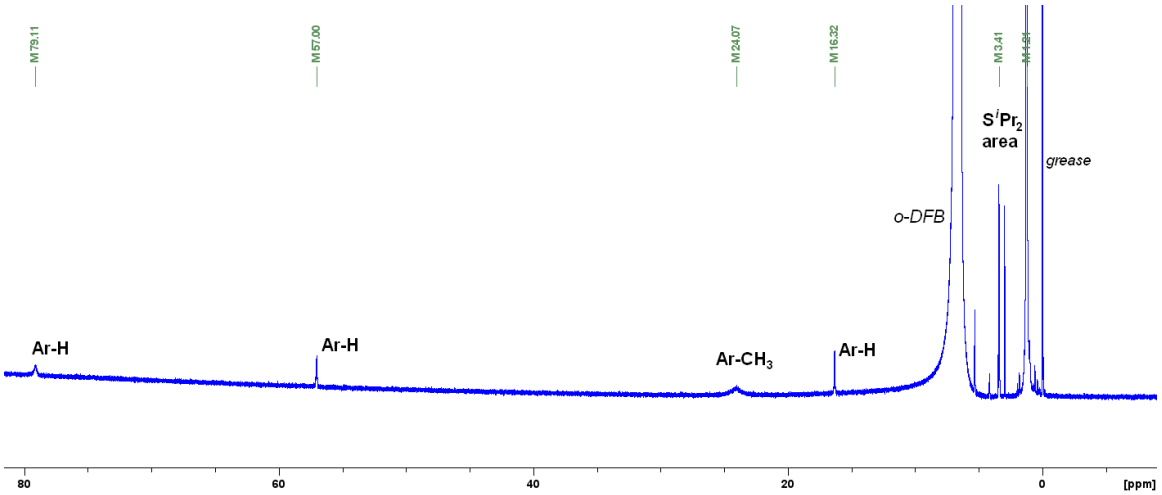

Figure S13 – Typical ^{1}H NMR (300MHz, 298K, *o*-DFB) of the crude mixture between $(bipyMe_2)NiCl_2$ and adduct **1-S^{i}Pr$_2$**.

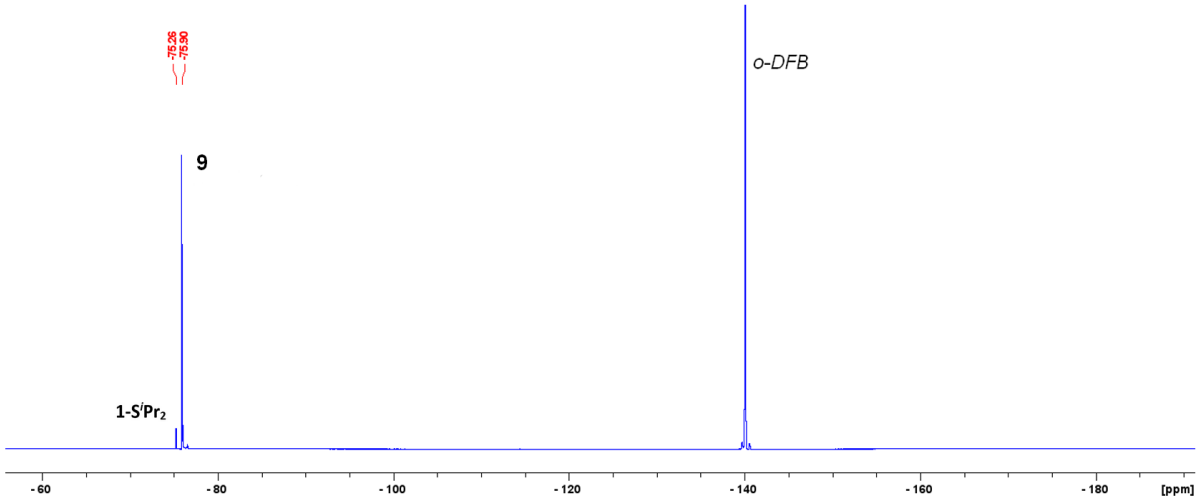

Figure S14 - Typical ^{19}F{^{1}H} NMR (282MHz, 298K, *o*-DFB) of the crude mixture between $(bipyMe_2)NiCl_2$ and adduct **1-S^{i}Pr$_2$**.

2. X-Ray diffraction data

	4	**1-S^{i}Pr$_2$**	**1-OPEt$_3$**	**5**
Formula	$C_{20}H_{10}Al_2F_{36}O_6$	$C_{18}H_{14}AlF_{27}O_3S$	$C_{18}H_{15}AlF_{27}O_4P$, C_6H_6	$C_{46}H_{26}Al_2F_{64}N_2NiO_7S$
M_r	1084.24	850.33	944.36	2079.42
Crystal system	Triclinic	Monoclinic	Monoclinic	Orthorombic
Space Group	$P\bar{1}$	$P2_1/n$	$C2/c$	$Pbca$
a (Å)	10.0323(19)	10.7911(4)	29.9848(19)	24.1444(13)
b (Å)	12.717(3)	20.6970(6)	15.1284(10)	21.0601(13)
c (Å)	14.470(3)	13.2908(4)	21.7400(13)	27.6394(17)
α (°)	93.105(7)	90	90	90
β (°)	90.120(7)	94.9310(11)	133.515(2)	90
γ (°)	105.550(6)	90	90	90
V (Å^3)	1775.6(6)	2957.43(17)	7151.7(8)	14054.2(14)
Z	2	4	8	8
ρ_{calc} (g.cm^{-3})	2.028	1.910	1.754	1.966
μ (mm^{-1})	0.309	0.333	0.274	0.550
F(000)	1056	1672	3744	8144
Crystal size (mm^3)	0.20x0.20x0.15	0.30x0.25x0.10	0.35x0.20x0.12	0.30x0.20x0.10
T (K)	193(2) K	193(2)	193(2)	193(2)
Meads reflns	48148	91952	110661	474478
Unique relfns (Rint)	5056 (0.1172)	7299 (0.0389)	7312 (0.1296)	18918 (0.0497)
Data/restaints/parameters	5056/1456/1157	7299/936/674	7312/1865/911	18918/2481/1659
GOF on F²	1.054	1.017	1.030	1.034
R_1[a] [I>2σ(I)]	0.1643	0.0432	0.0704	0.0509
wR_2[b] [all data]	0.5142	0.1249	0.2371	0.1529
Largest diff. peak and hole (e.Å^{-3})	1.128 & -0.899	0.334 & -0.311	0.603 & -0.725	1.007 & -0.601

	5-H_2O	**6^+[Al-F-Al]**	**6^+ [$Al(OR^F)_4$]**	**8**
Formula	$C_{28}H_{15}AlF_{36}N_2NiO_6$	$C_{58}H_{27}Al_2F_{64}N_2NiO_7P$	$C_{50}H_{27}AlF_{45}N_2NiO_5P$, ½ CH_2Cl_2	$C_{48}H_{24}Al_2Cl_4F_{54}N_4Ni_2O_6$
M_r	1245.11	2223.45	1728.63	2091.89
Crystal system	Monoclinic	Monoclinic	Triclinic	Monoclinic
Space Group	$P2_1/n$	$P2_1/n$	$P\bar{1}$	$P2_1/n$
a (Å)	11.5468(10)	11.2190(5)	11.7372(10)	10.9579(5)
b (Å)	30.466(3)	16.9651(9)	16.6414(13)	18.3013(9)
c (Å)	12.4220(11)	41.393(2)	16.7425(12)	17.8820(9)
α (°)	90	90	96.660(2)	90
β (°)	108.974(2)	90.0506(17)	97.005(2)	97.2316(18)
γ (°)	90	90	95.004(2)	90
V (Å^3)	4132.5(6)	7878.5(7)	3206.8(4)	3557.6(3)
Z	4	4	2	2
ρ_{calc} (g.cm^{-3})	2.001	1.875	1.790	1.953
μ (mm^{-1})	0.699	0.492	0.540	0.896
F(000)	2440	4360	1705	2048
Crystal size (mm^3)	0.12x0.08x0.04	0.25x0.22x0.07	0.20x0.18x0.05	0.20x0.20x0.20
T *(*K)	193(2) K	193(2)	153(2)	193(2)
Meads reflns	100938	292784	79642	166631
Unique relfns (Rint)	8424 (0.0791)	19535 (0.0562)	13065 (0.0832)	8823 (0.0861)
Data/restaints/parameters	8424/1434/1017	19535/2923/1826	13065/2672/1519	8823/453/653
GOF on F^2	1.034	1.033	1.020	1.017
R_1[a] [I>2σ(I)]	0.0434	0.0902	0.0898	0.0400
wR_2[b] [all data]	0.1196	0.2833	0.2828	0.1020
Largest diff. peak and hole (e.Å^{-3})	0.512 & -0.458	1.244 & -0.657	1.824 & -1.072	0.621 & -0.362

Stucture of complex 4 :

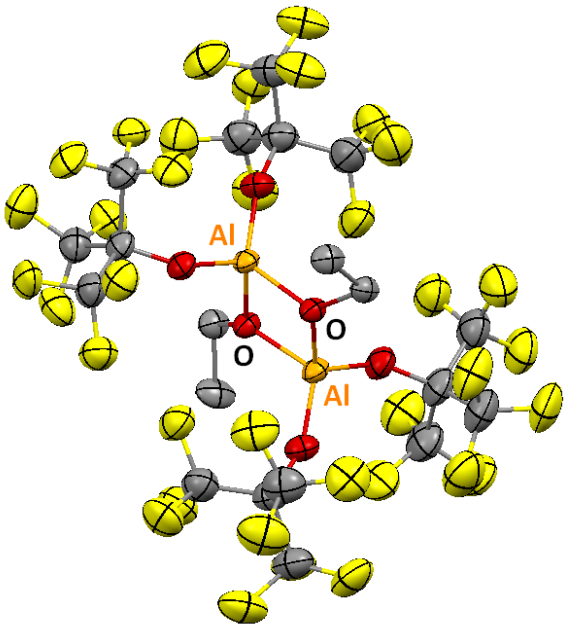

Figure S15 – Molecular structure of **4** in crystalline state. Thermal ellipsoids are drawn at 35% probability. H atoms are omitted for clarity.

Reactivity of **5** with water traces

The cationic complex **5**$^{+}$ is stable and soluble only in *o*-DFB and DCM. It is insoluble in non-polar solvents such as toluene or pentane. It decomposes to unknown products in THF and ACN. It is moreover sensitive to traces of water. Indeed, when a *o*-DFB solution of complex **5**$^{+}$ was kept in a screw cap NMR tube for days, colorless crystals formed. These crystals could be analyzed by XRD and gave the structure of compound **5-H$_2$O** [(bipyMe$_2$)Ni(OR^F)(H$_2$O)(μ-OH)(Al(OR^F)$_3$)] (**Figure S16**). The latter has a square-based pyramidal geometry around nickel (τ_5=0.04) and a tetrahedral geometry around aluminum (τ_4=0.95). Apparently, water traces react with complex **5**$^{+}$ by replacing the S^{i}Pr$_2$ ligand on nickel and reacting with the counterion [AlFAl]$^-$ to give the aluminate [(R^{F}O)$_3$AlOH]$^-$ (Al-O$_2$: 1.74 Å) which becomes coordinating (Ni-O$_2$: 2.03 Å). Nickel being much less electron deficient, the Ni-O$_3$R^F bond length is 1.97 Å, which is the longest we have observed.[1] The Ni-N distances (2.01 and 2.02 Å) are similar to complex **5**.

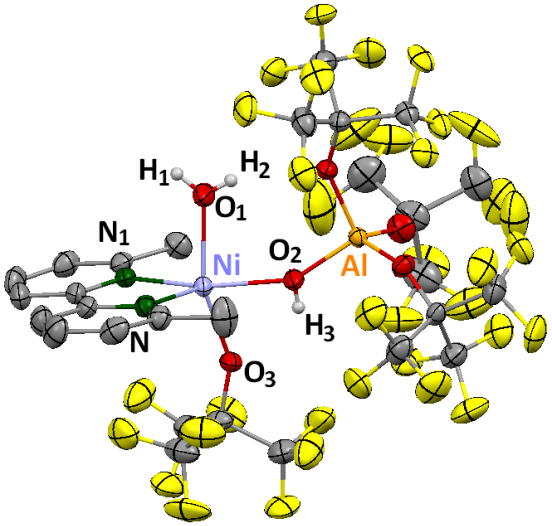

Figure S16 - Molecular structure of **5-H$_2$O** in crystalline state. Thermal ellipsoids are drawn at 50% probability. H atoms from the bipyridine ligand are omitted for clarity. Distances [Å] and angles [deg]: Ni-O$_1$:2.078(3) ; Ni-O$_2$: 2.032(2) ; Ni-O$_3$: 1.972(2) ; Al-O$_2$: 1.737(2) ; O$_1$-Ni-O$_3$: 156.09(11) ; O$_1$-Ni-O$_2$: 84.00(11) ; Ni-O$_2$-Al :150.75(15).

X-ray diffraction of **6⁺[Al-F-Al]⁻**:

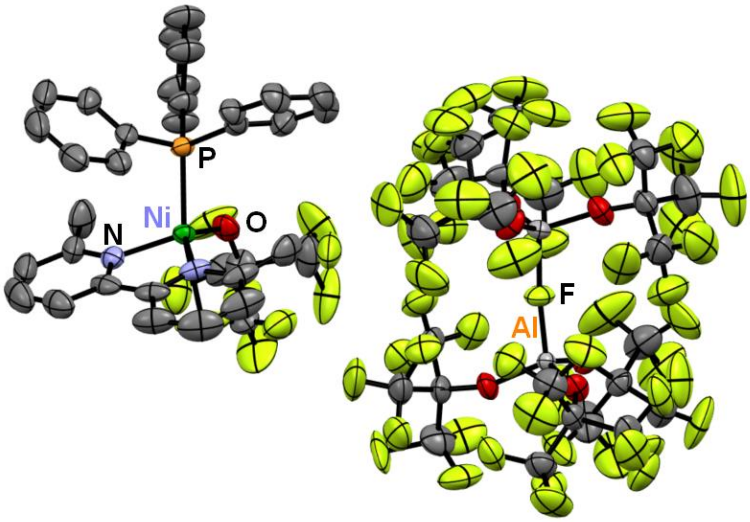

Figure S17 - Thermal ellipsoids are drawn at 50% probability. H atoms are omitted for clarity.

X-ray diffraction of **6⁺[Al(OR^F)$_4$]⁻**

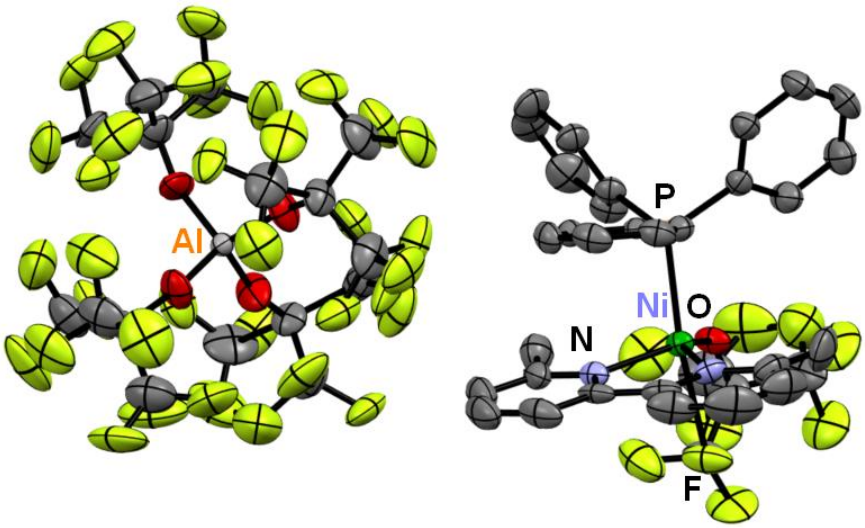

Figure S18 - Thermal ellipsoids are drawn at 50% probability. H atoms are omitted for clarity.

3. Computational details

Comparison of L→Al(OR^F)$_3$ Lewis adducts.[12]

Method used for mechanistic studies (functionals and bases chosen following benchmark studies – vide infra)

Geometry optimization were performed using Gaussian 09 (Revision D01)[13] at the B3PW91 level of hybrid density functional theory[14,16] adding D3(BJ) correction therm. [17,18] The geometries of all optimized structures are given in the .xyz file attached to the publication. The Ni atoms were represented by a LANL2TZ basis set.[19,20] The Al atoms were represented with the def2SV(P) basis set.[15] All other atoms (H, C, N, O, F, S) were represented by a 6-31G* basis set.[21–25] Frequency calculations on optimized geometries ensured that structures were minima (zero imaginary frequencies).

Theoretical benchmark for the determination of the appropriate functional/base(Ni) couple for mechanistic studies.

For this study, the XRD structure of compound **3** (bipyMe$_2$)Ni(OR^F)$_2$ was chosen as a reference.[1] Different functionals and bases were used to compare the distances and angles of compound **3**, measured by XRD. First, several functionals were evaluated (bases for all functionals: def2-tzvp + f for Ni and 6-31G* for the other atoms, Figure S19). The B3PW91 (Figure S19, right) functional appears appropriate, even if the differences with others remain minimal. The optimized structure with this functional presents angles and distances comparable to the XRD structure. All the functionals overestimated the O-Ni-O angle.

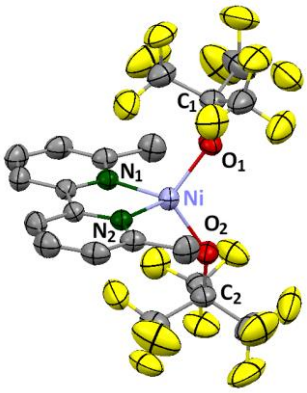

Base : Ni (def2-tzvp + f) / C, H, O, F, N (6-31G*)				
Functional	Ni-$O_{1/2}$ (Å)	Ni-$N_{1/2}$ (Å)	O_1-Ni-O_2 (°)	N_1-Ni-N_2 (°)
XRD	*1,893(2)*	*1,990(2)*	*109,73(11)*	*82,76(11)*
B3LYP	1,894	2,030	123,27	81,82
B3PW91	**1,889**	**2,015**	**122,67**	**81,96**
M06	1,884	2,016	128,39	81,99
M06L	1,902	2,013	124,49	81,23
M06-2X	1,908	2,068	128,24	79,88

Figure S19 – Left: XRD structure of **3**. Right: influence of different functionalities on the distances and angle of the cation of **3**.

However, the O_1-Ni-O_2 angle remains very high for all the considered functionals. We therefore chose to turn to a new base for nickel: LANL2TZ(f) which is used in some studies involving isolated Ni complexes, or even reaction intermediates involving Ni O bonds.[26–28] In this case, the data (distances and angles) are in slightly better agreement with the parameters determined by XRD (

Table **S1**). Again, the B3PW91 functional appears to fit best. A deviation of -0.010Å is observed for Ni-$O_{1/2}$ distances and +0.012Å for Ni-$N_{1/2}$. A difference with the XRD structure of more than 10° for the O_1-Ni-O_2 angle is however still present. A decrease of the deviation of the latter by 1.49° compared to the def2-tzvp + f basis (applied for Ni) indicates that the LANL2TZ(f) basis is more suitable.

Tests were performed by increasing the precision of the bases on the non-metallic atoms (C, H, N, O, F). The 6-311++G* base was thus used with the B3PW91 functional. Surprisingly, the values found are much less precise than with the 6-31G* base, in addition to a longer calculation time.

Table S1 - Influence of different functionals on the distances and angles of compound **3**.

Base : Ni (LANL2TZ(f)) / C, H, O, F, N (6-31G*)				
Fonctionnelle	Ni-$O_{1/2}$ (Å)	Ni-$N_{1/2}$ (Å)	O_1-Ni-O_2 (°)	N_1-Ni-N_2 (°)
XRD	*1,893(2)*	*1,990(2)*	*109,73(11)*	*82,76(11)*
B3LYP	1,887	2,024	121,44	81,94
B3PW91	**1,883**	**2,011**	**121,08**	**81,99**
M06L	1,895	2,003	122,89	81,54

In order to verify the importance of the theoretical O_1-Ni-O_2 angle value, a calculation varying the angle from 121° (theoretically determined value) to 105°, passing by 109.7° (experimentally found value), has been performed. What can be seen is that the energy difference is only 1.0 kcal.mol^{-1} between complex **3** with an O_1-Ni-O_2 angle of 121° and complex **3** with an angle of 110° (Figure S20). This shows that the value of the angle is not representative since the energy varies little with the value of this angle.

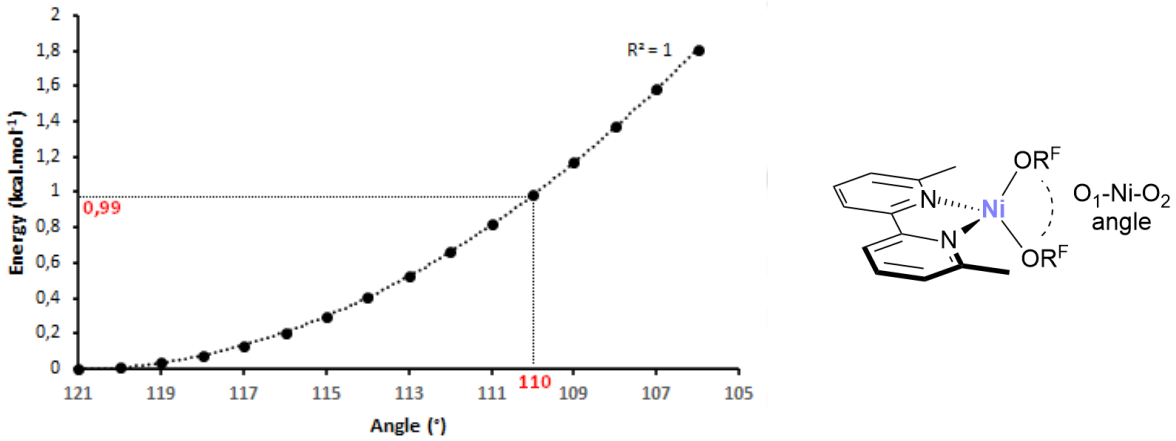

Figure S20 - Energy of compound **3** (calculated structure) according to the value of the O_1-Ni-O_2 angle.

The actual study involves cationic fragments comprising the [(bipyMe_2)Ni(OR^F)]$^+$ fragment **5**$^+$ and a substrate (epoxide, S^iPr_2). It is therefore necessary to ensure that the functional and the chosen bases are in adequation with the envisaged study. For this purpose, the fragment [(bipyMe_2)Ni(OR^F)(S^iPr_2)]$^+$ was optimized with the functional B3PW91, the base LANL2TZ(f) for Ni and 6-31G* for the other atoms. The obtained values are presented and compared with the values of the XRD structure of **5**$^+$ on the table in Figure S21. The calculated Ni-O distance is smaller than that of the RX structure by only 0.011 Å. The Ni-S and Ni-F distances are overestimated for the Ni-S (+0.072 Å) and underestimated for the Ni-F (-0.067 Å) without being unreasonable. The other calculated values are consistent with the experimental values. The chosen functional/basis set is thus appropriate for the systems under study here.

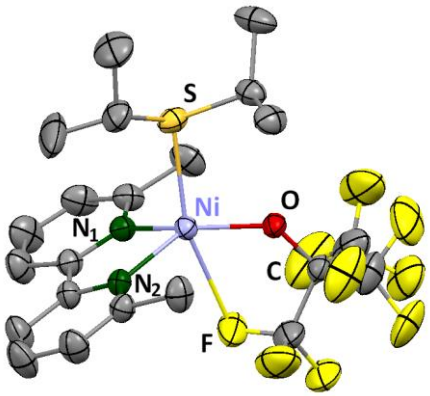

Functionnal : B3PW91. Base : Ni (LANL2TZ(f)) / C, H, O, F, N, S (6-31G*)		
$[(bipyMe_2)Ni(OR^F)(S^iPr_2)]^+$	XRD	DFT
Ni-O (Å)	1.873(2)	1.862
Ni-S (Å)	2.379(1)	2.451
Ni-F (Å)	2.530(1)	2.463
$Ni-N_1$ (Å)	2.010(2)	2.030
$Ni-N_2$ (Å)	2.008(2)	2.045
S-Ni-O (°)	93.38(5)	91.84
S-Ni-F (°)	162.27(5)	161.41
O-Ni-F (°)	71.35(7)	73.78
N_1-Ni-N_2 (°)	81.75(8)	81.36

Figure S21 – Left: DRX structure of the cationic part of **5**. Right: comparative table of experimental (XRD) and theoretical (DFT) $[(bipyMe_2)Ni(OR^F)(S^iPr_2)]^+$ distances and angles.

4. References

[1] J. Petit, N. Saffon-Merceron, L. Magna, N. Mézailles, *Organometallics* **2021**, *40*, 4133–4142.

[2] K. Yamaguchi, *J. Mass Spectrom.* **2003**, *38*, 473–490.

[3] U. Bruker, SADABS, Bruker AXS Inc., Madison, Wisconsin, **2008**.

[4] G. M. Sheldrick, *Acta Crystallogr. Sect. A Found. Crystallogr.* **2015**, *71*, 3–8.

[5] A. L. Spek, *J. Appl. Crystallogr.* **2003**, *36*, 7–13.

[6] T. A. Engesser, M. R. Lichtenthaler, M. Schleep, I. Krossing, *Chem. Soc. Rev.* **2016**, *45*, 789–799.

[7] A. Kraft, N. Trapp, D. Himmel, H. Böhrer, P. Schlüter, H. Scherer, I. Krossing, *Chem. - A Eur. J.* **2012**, *18*, 9371–9380.

[8] A. Martens, P. Weis, M. C. Krummer, M. Kreuzer, A. Meierhöfer, S. C. Meier, J. Bohnenberger, H. Scherer, I. Riddlestone, I. Krossing, *Chem. Sci.* **2018**, *9*, 7058–7068.

[9] M. Schleep, C. Hettich, J. Velázquez Rojas, D. Kratzert, T. Ludwig, K. Lieberth, I. Krossing, *Angew. Chemie - Int. Ed.* **2017**, *56*, 2880–2884.

[10] S. C. Meier, A. Holz, J. Kulenkampff, A. Schmidt, D. Kratzert, D. Himmel, D. Schmitz, E. W. Scheidt, W. Scherer, C. Bülow, et al., *Angew. Chemie - Int. Ed.* **2018**, *57*, 9310–9314.

[11] D. S. Mcguinness, A. J. Rucklidge, R. P. Tooze, A. M. Z. Z. Slawin, *Organometallics* **2007**, *26*, 2561.

[12] A. Kraft, J. Beck, G. Steinfeld, H. Scherer, D. Himmel, I. Krossing, *Organometallics* **2012**, *31*, 7485–7491.

[13] Frisch, M. J.; Trucks, G. W.; Schlegel, H. B.; Scuseria, G. E.; Robb, M. A.; Cheeseman, J. R.; Scalmani, G.; Barone, V.; Mennucci, B.; Petersson, G. A.; Nakatsuji, H.; Caricato, M.; Li, X.; Hratchian, H. P.; Izmaylov, A. F.; Bloino, J.; Zheng, G.; Sonnenb, **2013**.

[14] A. D. Becke, *J. Chem. Phys.* **1988**, *38*, 3098–3100.

[15] F. Weigend, R. Ahlrichs, F. K. Gmbh, *Phys. Chem. Chem. Phys.* **2005**, *7*, 3297–3305.

[16] A. D. Becke, *J. Chem. Phys.* **1993**, *98*, 5648–5652.

[17] S. Grimme, J. Antony, S. Ehrlich, H. Krieg, *J. Chem. Phys.* **2010**, *132*, DOI 10.1063/1.3382344.

[18] S. Grimme, S. Ehrlich, L. Goerick, *J. Comput. Chem.* **2011**, *32*, 1456–1465.

[19] P. J. Hay, W. R. Wadt, *J. Chem. Phys.* **1985**, *82*, 270–283.

[20] L. E. Roy, P. J. Hay, R. L. Martin, *J. Chem. Theory Comput.* **2008**, *4*, 1029–1031.

[21] R. Ditchfield, W. J. Hehre, J. A. Pople, *J. Chem. Phys.* **1971**, *54*, 720–723.

[22] W. J. Hehre, K. Ditchfield, J. A. Pople, *J. Chem. Phys.* **1972**, *56*, 2257–2261.

[23] P. C. Hariharan, J. A. Pople, *Theor. Chim. Acta* **1973**, *28*, 213–222.

[24] M. M. Francl, W. J. Pietro, W. J. Hehre, J. S. Binkley, M. S. Gordon, D. J. DeFrees, J. A. Pople, *J. Chem. Phys.* **1982**, *77*, 3654–3665.

[25] M. S. Gordon, S. J. Binkley, J. A. Pople, W. J. Pietro, W. J. Hehre, **1982**, *104*, 2797–2803.

[26] M. Sheng, N. Jiang, S. Gustafson, B. You, D. H. Ess, Y. Sun, *Dalt. Trans.* **2015**, *44*, 16247–16250.

[27] S. K. Sontag, J. A. Bilbrey, N. E. Huddleston, G. R. Sheppard, W. D. Allen, J. Locklin, *J. Org. Chem.* **2014**, *79*, 1836–1841.

[28] H. Xie, Q. Sun, G. Ren, Z. Cao, *J. Org. Chem.* **2014**, *79*, 11911–11921.